

A Posteriori Error Estimates for Elliptic Variational Inequalities

Ralf Kornhuber

*Weierstraß-Institut für Angewandte Analysis und Stochastik Berlin
Mohrenstraße 39, D-10117 Berlin, Fed. Rep. of Germany*

Abstract. We derive hierarchical a posteriori error estimates for elliptic variational inequalities. The evaluation amounts to the solution of corresponding scalar local subproblems. We derive some upper bounds for the effectivity rates and the numerical properties are illustrated by typical examples.

Key words: free boundary problems, adaptive finite element methods, a posteriori error estimates

AMS (MOS) subject classifications: 65N30, 65N55, 35J85

1 Introduction

A posteriori error estimates play a crucial role in the approximate solution of partial differential equations by adaptive finite element methods. In this paper we will consider *hierarchical error estimates* which are resulting from the following two steps.

- Discretize the defect problem with respect to an enlarged space.
- Localize the discrete defect problem by domain decomposition.

The first appearance of hierarchical error estimates that we know is in the work of Zienkiewicz et al. [1] in the early eighties. The intimate relation to preconditioning was made explicit by Deuffhard, Leinen, and Yserentant [2]. Recently, it turned out that the hierarchical approach allows a unified view on a variety of apparently different concepts (cf. Bornemann, Erdmann, and Kornhuber [3, 4] and Verfürth [5, 6]).

Bank and Smith [7] have extended hierarchical error estimates from the elliptic selfadjoint case to a variety of other situations including smooth nonlinear problems. Here we will concentrate on non-smooth optimization problems as arising in the fixed-domain formulation of certain free boundary problems. Obstacle problems or semi-discretized Stefan problems are typical examples. As Newton-type linearization cannot be used, we will apply the hierarchical concept to the given nonlinear problem directly. This requires some care in the localization of the discrete defect problem. A straightforward approach was applied successfully to a special obstacle problem arising from semiconductor device simulation [8, 9]. However, it turned out in the subsequent analysis and numerical experiments (cf. Hoppe and Kornhuber [10]) that in general the resulting error estimate is not robust. In particular, there are no finite upper bounds of the effectivity rates because the localized defect problem may have a vanishing solution even if the solution of the discrete defect problem is not zero.

In the present paper this problem is remedied by using a diagonal scaling of the discrete defect problem. In this way, the original global problem is decomposed in a number of one-dimensional subproblems. The quality of the resulting error estimate relies on the condition that the solutions of the discrete defect problem and of the decoupled version are *high frequency* functions (cf. Theorem 4.1). This condition is satisfied in the linear selfadjoint case where we can prove optimal bounds for the effectivity rates. We refer to similar properties of *cascadic iterations* (cf. Deuffhard [11], Shaidurov [12] and Bornemann and Deuffhard [13]). In the general nonlinear case our present analysis only gives exponential bounds. On the other hand, numerical experiments showed similar effectivity rates as for related linear problems

so that these pessimistic theoretical results may still be improved.

2 The Continuous Problem and its Discretization

Let Ω be a bounded polygonal domain in the Euclidean space \mathbb{R}^2 . We consider the optimization problem

$$u \in H_0^1(\Omega) : \quad \mathcal{J}(u) + \phi(u) \leq \mathcal{J}(v) + \phi(v), \quad v \in H_0^1(\Omega). \quad (2.1)$$

Other boundary conditions of Neumann or mixed type and the case of three space dimensions can be treated in a similar way [3, 4]. The quadratic functional

$$\mathcal{J}(v) = \frac{1}{2}a(v, v) - \ell(v) \quad (2.2)$$

is induced by a continuous, symmetric and $H_0^1(\Omega)$ -elliptic bilinear form $a(\cdot, \cdot)$ and a linear functional $\ell \in H^{-1}(\Omega)$. The convex functional $\phi : H_0^1(\Omega) \rightarrow \mathbb{R} \cup \{+\infty\}$ of the form

$$\phi(v) = \int_{\Omega} \Phi(v(x))dx, \quad (2.3)$$

is generated by a scalar convex function Φ . We assume that Φ is chosen in such a way that ϕ is lower semi-continuous and proper (i.e. $\phi \not\equiv +\infty$ and $\phi(v) > -\infty$, $v \in H_0^1(\Omega)$). To fix the ideas, we give two typical examples. The first one is an obstacle problem generated by the indicator function

$$\Phi(z) = \begin{cases} 0, & \text{if } z \leq \theta_0 \\ +\infty, & \text{if } z > \theta_0 \end{cases} \quad (2.4)$$

with some upper obstacle $\theta_0 \in \mathbb{R}$. The other example is resulting from the implicit time discretization of a two-phase Stefan problem. Denoting $z_- = -\min\{z, 0\}$ and $z_+ = \max\{z, 0\}$ the piecewise quadratic function

$$\Phi(z) = \frac{1}{2}a_1(z - \theta_0)_-^2 + s_1(z - \theta_0)_- + \frac{1}{2}a_2(z - \theta_0)_+^2 + s_2(z - \theta_0)_+ \quad (2.5)$$

with non-negative constants $a_1, a_2, s_1, s_2 \in \mathbb{R}$ now stands for the potential of the generalized enthalpy. For positive latent heat $s_1 + s_2$ the derivative of Φ is discontinuous at the phase transition temperature $\theta_0 \in \mathbb{R}$. A variety of other examples can be found in the monographs of Crank [14], Duvaut and Lions [15], Glowinski [16] and the literature cited therein.

It is well-known (cf. e.g. [16]) that (2.1) admits a unique solution and can be equivalently rewritten as the following variational inequality of the second kind

$$u \in H_0^1(\Omega) : \quad a(u, v - u) + \phi(v) - \phi(u) \geq \ell(v - u), \quad v \in H_0^1(\Omega). \quad (2.6)$$

Let \mathcal{T} be a consistent triangulation of Ω . The sets of interior nodes and edges are called \mathcal{N} and \mathcal{E} , respectively. Discretizing (2.6) by continuous, piecewise linear finite elements $\mathcal{S} \subset H_0^1(\Omega)$, we obtain the finite dimensional problem

$$u_{\mathcal{S}} \in \mathcal{S} : a(u_{\mathcal{S}}, v - u_{\mathcal{S}}) + \phi_{\mathcal{S}}(v) - \phi_{\mathcal{S}}(u_{\mathcal{S}}) \geq \ell(v - u_{\mathcal{S}}), \quad v \in \mathcal{S}. \quad (2.7)$$

Observe that the functional ϕ is approximated by the \mathcal{S} -interpolation of the integrand $\Phi(v)$, giving

$$\phi_{\mathcal{S}}(v) = \int_{\Omega} \sum_{p \in \mathcal{N}} \Phi(v(p)) \lambda_p(x) dx, \quad v \in \mathcal{S}, \quad (2.8)$$

where $\Lambda = \{\lambda_p \mid p \in \mathcal{N}\}$ stands for the nodal basis of \mathcal{S} . Of course, the discrete problem (2.7) is uniquely solvable. For convergence results we refer for example to Glowinski [16], Brezzi et al. [17], and Elliot [18]. The efficient iterative solution of (2.7) by monotone multigrid methods has been considered by Kornhuber [19, 20].

3 Discrete Defect Problems

Assume that $\tilde{u} \in \mathcal{S}$ is an approximation of the finite element solution $u_{\mathcal{S}}$ of (2.7). Usually \tilde{u} is produced by some iterative solver. We want to derive upper and lower bounds for the *approximation error* $\|u - \tilde{u}\|$ with respect to the energy norm $\|\cdot\| = a(\cdot, \cdot)^{1/2}$. Note that the *algebraic error* $\|u_{\mathcal{S}} - \tilde{u}\|$ may interfere with the *discretization error* $\|u - u_{\mathcal{S}}\|$.

Observe that the desired correction $e = u - \tilde{u}$ is the unique solution of the defect problem

$$e \in H_0^1(\Omega) : \quad a(e, v - e) + \psi(v) - \psi(e) \geq r(v - e), \quad v \in H_0^1(\Omega), \quad (3.1)$$

where we have used the translated functional ψ defined by

$$\psi(v) = \phi(\tilde{u} + v) = \int_{\Omega} \Phi(\tilde{u}(x) + v(x)) dx, \quad v \in H_0^1(\Omega),$$

and the residual

$$r = \ell - a(\tilde{u}, \cdot) \in H^{-1}(\Omega).$$

To discretize the continuous defect problem (3.1), we introduce the finite element space of continuous, piecewise quadratic functions $\mathcal{Q} \subset H_0^1(\Omega)$, spanned by the nodal basis

$$\Lambda_{\mathcal{Q}} = \{\lambda_p^{\mathcal{Q}} \mid p \in \mathcal{N}_{\mathcal{Q}}\}.$$

Here we have set $\mathcal{N}_{\mathcal{Q}} = \mathcal{N} \cup \mathcal{N}_{\mathcal{E}}$ and $\mathcal{N}_{\mathcal{E}}$ consists of the midpoints of the interior edges. Interpolating $\Phi(\tilde{u} + v)$ by piecewise quadratic finite elements, we obtain the approximation

$$\psi_{\mathcal{Q}}(v) = \int_{\Omega} \sum_{p \in \mathcal{N}_{\mathcal{Q}}} \Phi(\tilde{u}(p) + v(p)) \lambda_p^{\mathcal{Q}}(x) dx, \quad v \in \mathcal{Q},$$

of the defect functional ψ . Then $e_{\mathcal{Q}} \in \mathcal{Q}$ is the unique solution of the *discrete defect problem*

$$e_{\mathcal{Q}} \in \mathcal{Q} : \quad a(e_{\mathcal{Q}}, v - e_{\mathcal{Q}}) + \psi_{\mathcal{Q}}(v) - \psi_{\mathcal{Q}}(e_{\mathcal{Q}}) \geq r(v - e_{\mathcal{Q}}), \quad v \in \mathcal{Q}. \quad (3.2)$$

Correcting \tilde{u} by $e_{\mathcal{Q}}$ we obtain the *piecewise quadratic approximation*

$$u_{\mathcal{Q}} = \tilde{u} + e_{\mathcal{Q}} \in \mathcal{Q}$$

with respect to the triangulation \mathcal{T} .

Note that there are other interesting ways of extending the underlying finite element space \mathcal{S} , in particular in the case of three space dimensions [4].

We now investigate the *effect of discretization* on the continuous defect problem (3.1).

Theorem 3.1 *Assume that u_Q provides a better approximation than \tilde{u} in the sense that*

$$\|u - u_Q\| \leq \beta \|u - \tilde{u}\| \quad (3.3)$$

holds with some $\beta < 1$. Then we have the estimates

$$(1 + \beta)^{-1} \|e_Q\| \leq \|u - \tilde{u}\| \leq (1 - \beta)^{-1} \|e_Q\|. \quad (3.4)$$

Proof. The proof follows immediately from the triangle inequality. ■

The crucial condition (3.3) with $\beta = \beta_s / (1 - \beta_a) < 1$ is a consequence of the *saturation assumption*

$$\|u - u_Q\| \leq \beta_s \|u - u_S\|, \quad \beta_s < 1, \quad (3.5)$$

and the *algebraic accuracy assumption*

$$\|u_S - \tilde{u}\| \leq \beta_a \|u - u_S\|, \quad \beta_a < 1 - \beta_s. \quad (3.6)$$

The saturation assumption (3.5) states that the larger finite element space Q provides a better approximation than the original space S . For sufficiently regular problems the piecewise quadratic solution u_Q is even an approximation of higher order (see for instance [17]). In this case (3.5) clearly holds for sufficiently fine triangulations. On the other hand, there are simple examples showing that (3.5) may be violated, if the mesh is not properly chosen. In this sense reliable a posteriori error estimates still involve a certain amount of *a priori information*.

The algorithmic realization of the algebraic accuracy assumption (3.6) will be discussed in the final section.

In the case of elliptic selfadjoint problems, (3.6) is not needed and the saturation assumption (3.5) is even equivalent to the upper estimate in (3.4) with $\beta = \beta_s$. We refer to [4] for details.

4 Preconditioned Discrete Defect Problems

In general, the solution of the discrete defect problem (3.2) is not available at reasonable computational cost. This motivates further simplifications which should preserve lower and upper bounds of the form (3.4).

Extending well-known results from the elliptic selfadjoint case [2, 3, 4, 7], we will now investigate the *effect of preconditioning* on the solution e_Q of (3.2). For this reason we consider the variational inequality

$$e_b \in Q : \quad b(e_b, v - e_b) + \psi_Q(v) - \psi_Q(e_b) \geq r(v - e_b), \quad v \in Q, \quad (4.1)$$

with some symmetric and positive definite bilinear form $b(\cdot, \cdot)$ on Q . Observe that the *preconditioned defect problem* (4.1) is uniquely solvable and that the preconditioner $b(\cdot, \cdot)$ induces the norm $|\cdot| = b(\cdot, \cdot)^{1/2}$ on Q .

Theorem 4.1 *Assume that the norm equivalence*

$$\gamma_0 b(v, v) \leq a(v, v) \leq \gamma_1 b(v, v), \quad v \in \text{span}\{e_Q, e_b\}, \quad (4.2)$$

holds with positive constants γ_0, γ_1 . Then we have the estimates

$$c_0 |e_b|^2 \leq \|e_Q\|^2 \leq c_1 |e_b|^2 \quad (4.3)$$

with $c_0 = (\gamma_0^{-1} + 2\gamma_1(1 + \gamma_0^{-1}))^{-1}$ and $c_1 = \gamma_1 + 2\gamma_0^{-1}(1 + \gamma_1)$.

Proof. By symmetry arguments it is sufficient to establish only the right inequality in (4.3). Inserting $v = e_b$ in the original discrete defect problem (3.2), we obtain

$$\|e_Q\|^2 \leq a(e_Q, e_b) + \psi_Q(e_b) - \psi_Q(e_Q) + r(e_Q - e_b).$$

Now the inequality $2a(e_Q, e_b) \leq \|e_Q\|^2 + \|e_b\|^2$ and (4.2) yield

$$\|e_Q\|^2 \leq \gamma_1 |e_b|^2 + 2(\psi_Q(e_b) - \psi_Q(e_Q) + r(e_Q - e_b)). \quad (4.4)$$

It remains to show that

$$\psi_Q(e_b) - \psi_Q(e_Q) + r(e_Q - e_b) \leq \gamma_0^{-1}(\gamma_1 + 1)|e_b|^2. \quad (4.5)$$

Inserting $v = e_Q$ in (4.1) and using the Cauchy–Schwarz inequality, we get

$$\psi_Q(e_b) - \psi_Q(e_Q) + r(e_Q - e_b) \leq |e_b| |e_Q - e_b|$$

so that (4.5) follows from

$$|e_Q - e_b| \leq \gamma_0^{-1}(1 + \gamma_1)|e_b|. \quad (4.6)$$

In order to prove (4.6), we insert $v = e_b$ in (3.2) and $v = e_Q$ in the preconditioned problem (4.1). Adding the two resulting inequalities we obtain

$$a(e_Q, e_b - e_Q) + b(e_b, e_Q - e_b) \geq 0$$

which can be reformulated as

$$\|e_b - e_Q\|^2 \leq a(e_b, e_b - e_Q) - b(e_b, e_b - e_Q).$$

The assertion now follows from the Cauchy–Schwarz inequality and (4.2). ■

In the light of Theorem 4.1, we are left with the problem to select a preconditioner $b(\cdot, \cdot)$ which combines reasonable constants γ_0, γ_1 with a cheap evaluation of e_b . In analogy to the linear selfadjoint case one might be tempted to construct a preconditioner based on the hierarchical splitting

$$Q = S \oplus \mathcal{V} \tag{4.7}$$

where the difference space $\mathcal{V} = \text{span}\{\lambda_p^Q \mid p \in \mathcal{N}_\mathcal{E}\}$ consists of the quadratic bubble functions associated with the edges \mathcal{E} (cf. e.g. [2, 3, 4, 7]). However, in contrast to the linear case the unknowns now become coupled with respect to the functional ψ_Q as soon as the hierarchical representation is used. Even in simple cases, this coupling cannot be ignored without loosing the reliability of the resulting error estimate [10]. On the other hand, the coupled preconditioned problem is still not solvable with reasonable computational effort.

To find a way out of this dilemma, observe that the constants γ_0, γ_1 appearing in the crucial estimate (4.3) depend only on the *local quality* of the preconditioner $b(\cdot, \cdot)$ on the subspace $\text{span}\{e_Q, e_b\} \subset Q$. As a consequence, we can expect good results even from very simple preconditioners like the diagonal scaling

$$b(v, w) = \sum_{p \in \mathcal{N}_Q} v(p)w(p)a(\lambda_p^Q, \lambda_p^Q), \quad v, w \in Q, \tag{4.8}$$

if e_Q and e_b are *high frequency* functions.

In addition, the preconditioned defect equation (4.1) resulting from the diagonal scaling (4.8) consists of independent *local subproblems* for the nodal values of e_b . In many applications (involving for example a piecewise quadratic scalar function Φ) these sub-problems can be solved explicitly.

The Theorems 3.1 and 4.1 immediately provide (quite pessimistic) upper bounds for the effectivity rates of the resulting error estimate which increase exponentially with the refinement level. However, this implies at least that the localization preserves a *non vanishing* error estimate $|e_b| \neq 0$, if e_Q is not zero. Related previous error estimates do not have this property [10].

In the special case of linear elliptic problems the above results can be significantly improved.

Proposition 4.1 *Let the preconditioner $b(\cdot, \cdot)$ be given by (4.8). Assume that $\Phi \equiv 0$ and that the discrete problem (2.7) has been solved exactly, i.e. $\tilde{u} = u_S$. Then the estimates (4.3) hold with constants depending only on the ellipticity of $a(\cdot, \cdot)$ and on the shape regularity of \mathcal{T} .*

Proof. Let us consider the hierarchical splitting (4.7). For given $v \in \mathcal{Q}$ the superscripts \mathcal{S} and \mathcal{V} will indicate the contributions $v^{\mathcal{S}} \in \mathcal{S}$ and $v^{\mathcal{V}} \in \mathcal{V}$ of the unique decomposition $v = v^{\mathcal{S}} + v^{\mathcal{V}}$. We will make use of the bilinear forms

$$\hat{a}(v, w) = a(v^{\mathcal{S}}, w^{\mathcal{S}}) + \sum_{p \in \mathcal{N}_{\varepsilon}} v^{\mathcal{V}}(p) w^{\mathcal{V}}(p) a(\lambda_p^{\mathcal{Q}}, \lambda_p^{\mathcal{Q}})$$

and

$$\hat{b}(v, w) = \sum_{p \in \mathcal{N}} v^{\mathcal{S}}(p) w^{\mathcal{S}}(p) a(\lambda_p^{\mathcal{Q}}, \lambda_p^{\mathcal{Q}}) + \sum_{p \in \mathcal{N}_{\varepsilon}} v^{\mathcal{V}}(p) w^{\mathcal{V}}(p) a(\lambda_p^{\mathcal{Q}}, \lambda_p^{\mathcal{Q}})$$

defined on \mathcal{Q} . Observe that both preconditioners are based on the hierarchical splitting (4.7) and subsequent diagonalization. Using the standard affine transformation technique in a similar way as for example in [4, 2], it can be shown that the norm equivalences

$$b(v, v) \asymp \hat{b}(v, v), \quad \hat{a}(v, v) \asymp a(v, v) \quad (4.9)$$

hold for all $v \in \mathcal{Q}$. Here the abbreviation $x \asymp y$ stands for the estimates $cy \leq x \leq Cy$ with constants c, C depending only on the ellipticity of $a(\cdot, \cdot)$ and on the shape regularity of \mathcal{T} . Using the preconditioners $\hat{a}(\cdot, \cdot)$ and $\hat{b}(\cdot, \cdot)$ in the preconditioned defect problem (4.1), we obtain the corrections $e_{\hat{a}}$ and $e_{\hat{b}}$, respectively. Now the estimates

$$|e_b|^2 \asymp \hat{b}(e_{\hat{b}}, e_{\hat{b}}), \quad \hat{a}(e_{\hat{a}}, e_{\hat{a}}) \asymp \|e_{\mathcal{Q}}\|^2 \quad (4.10)$$

are an immediate consequence of Theorem 4.1. The crucial question is how to relate $\hat{b}(e_{\hat{b}}, e_{\hat{b}})$ to $\hat{a}(e_{\hat{a}}, e_{\hat{a}})$.

Here we make heavily use of the assumption $\Phi \equiv 0$. In this case the discrete defect problem (3.2) reduces to the variational equality

$$e_{\mathcal{Q}} \in \mathcal{Q} : \quad a(e_{\mathcal{Q}}, v) = r(v), \quad v \in \mathcal{Q}. \quad (4.11)$$

Replacing $a(\cdot, \cdot)$ by the preconditioner $\hat{b}(\cdot, \cdot)$, the linear and the quadratic contribution of $e_{\hat{b}} = e_{\hat{b}}^{\mathcal{S}} + e_{\hat{b}}^{\mathcal{V}}$ are completely decoupled. The same happens if the other hierarchical preconditioner $\hat{a}(\cdot, \cdot)$ is used. Applying in addition that $r(v) = 0$ holds for all $v \in \mathcal{S}$ (a consequence of the second assumption $\tilde{u} = u_S$), we get

$$e_{\hat{b}}^{\mathcal{S}} = e_{\hat{a}}^{\mathcal{S}} = 0, \quad e_{\hat{b}}^{\mathcal{V}} = e_{\hat{a}}^{\mathcal{V}}. \quad (4.12)$$

This clearly yields $\hat{b}(e_{\hat{b}}, e_{\hat{b}}) = \hat{a}(e_{\hat{a}}, e_{\hat{a}})$ and the assertion follows from (4.10).

■

The above result reminds to related properties of *cascadic iterations* as introduced by Deuffhard [11] and further analyzed by Shaidurov [12] and Bornemann and Deuffhard [13]. A similar estimate can be also found in [2].

Proposition 4.1 can be extended to variational inequalities under severe restrictions on the behavior of the discrete free boundary [21]. The main difficulty is that the equations (4.12) are no longer valid because now the linear and the quadratic parts of $e_{\hat{b}}$ and $e_{\hat{a}}$ *remain coupled* with respect to the nonlinear functional ψ_Q . This basic problem was already mentioned above.

Nevertheless Proposition 4.1 gives some motivation to assume that the correction e_Q is a high frequency function. Then Theorem 4.1 assures that $|e_{\hat{b}}|$ provides reasonable lower and upper bounds for the exact correction $\|e_Q\|$. This heuristic reasoning is strengthened by our numerical experiments reported below.

To increase the robustness (and unfortunately the computational costs) of the a posteriori error estimation one may consider the iterative solution of the discrete defect problem (3.2) as suggested in [21].

5 Numerical Experiments

A posteriori estimates of the approximation error are typically used as part of an adaptive multilevel method in order to provide stopping criteria for the complete algorithm and local error indicators for the adaptive refinement. Based on the *global* estimate $|e_b|$ as resulting from (4.1) with diagonal scaling (4.8) we select *local* error indicators as follows.

Using the hierarchical splitting (4.7) we decompose e_b according to

$$e_b = e_b^{\mathcal{S}} + e_b^{\mathcal{V}}, \quad e_b^{\mathcal{S}} \in \mathcal{S}, \quad e_b^{\mathcal{V}} \in \mathcal{V}.$$

Here $e_b^{\mathcal{S}}$ and $e_b^{\mathcal{V}}$ represent the low and high frequency parts of e_b . In analogy to the linear selfadjoint case we want to refine the given triangulation \mathcal{T} in such regions where the high frequency contributions deteriorate the overall accuracy. Hence, the local contributions η_p ,

$$\eta_p = e_b^{\mathcal{V}}(p)^2 a(\lambda_p^{\mathcal{Q}}, \lambda_p^{\mathcal{Q}}), \quad p \in \mathcal{N}_{\mathcal{E}},$$

of $|e_b^{\mathcal{V}}|^2 = \sum_{p \in \mathcal{N}_{\mathcal{E}}} \eta_p$ are used as *local error indicators*. If η_p exceeds a certain threshold $\bar{\eta}$ then the two triangles containing p are marked for refinement. The threshold $\bar{\eta}$ is computed by extrapolation [22]. Marked triangles are subdivided into four congruent subtriangles. Additional refinement may be necessary for structural reasons. See for example Bank [23] or Deuffhard, Leinen, and Yserentant [2] for further information.

An *adaptive cycle* consists of discretization, iterative solution and adaptive refinement of the given triangulation. An adaptive algorithm is producing a sequence of triangulations \mathcal{T}_j , of corresponding approximations \tilde{u}_j and of error estimates $|e_b^j|$, $j = 0, \dots$, by inductive application of adaptive cycles to an intentionally coarse initial triangulation \mathcal{T}_0 . The algorithm stops, if the estimated error is bounded by some prescribed accuracy TOL,

$$|e_b^j| \leq \text{TOL}. \tag{5.1}$$

The *refinement level* j counts the number of adaptive cycles while the *refinement depth* of \mathcal{T}_j denotes the maximal number of successive refinements applied to an initial triangle $t \in \mathcal{T}_0$. For selfadjoint elliptic problems a theoretical justification of a similar adaptive approach was recently given by Dörfler [24].

An estimate of the *relative approximation error* is given by $100 \cdot |e_b^j| / \|\tilde{u}_j\| \%$. In the following numerical examples, we approximate the solution with an (estimated) accuracy of 5%. Equivalently, the algorithm stops, if (5.1) is satisfied with $\text{TOL} = 0.05 \cdot \|\tilde{u}_j\|$.

The discrete problems (2.7) occurring on each refinement level are solved iteratively using monotone multigrid methods as introduced by Kornhuber

[19, 20]. Denoting the iterates on level j by u_j^0, u_j^1, \dots , the *relative algebraic error* of the ν -th iterate is estimated by $100 \cdot \|u_j^{\nu+1} - u_j^\nu\| / \|u_j^{\nu+1}\| \%$. We refer to [21] for a theoretical justification. The iterate $\tilde{u}_j := u_j^{\nu+1}$ is accepted as soon as the estimated relative algebraic error of u_j^ν is less than 0.5% (assuming that $u_j^{\nu+1}$ is even more accurate than u_j^ν).

Ignoring constants, let us for the moment assume that our estimates are representing the algebraic and the approximation error exactly. Then the above stopping criterion for the algebraic solver clearly implies the algebraic accuracy assumption (3.6) with $\beta_a = 1/9$ as long as the relative approximation error is greater than 5%, i.e. until the final level is reached. On the final level this inequality still holds with $\beta_a = 1/4$, if the relative approximation error on this level is still greater than 2.5%, i.e. if it is not reduced by more than a factor of 2 in the final refinement step. This is a reasonable assumption, because asymptotically the discretization error is well-known to decrease at most linearly with the maximal stepsize which in turn can be only halved in each refinement step.

The implementation was carried out in the framework of a recent C++ version of the finite element toolbox KASKADE [25].

Example 5.1: Obstacle Problem We consider the numerical solution of the obstacle problem

$$u \in \mathcal{K} : \quad \mathcal{J}(u) \leq \mathcal{J}(v), \quad v \in \mathcal{K}, \quad (5.2)$$

where \mathcal{J} is defined in (2.2) and the closed convex set \mathcal{K} is given by

$$\mathcal{K} = \{v \in H_0^1(\Omega) \mid v(x) \leq \varphi(x) \text{ a.e. in } \Omega\}$$

with some obstacle function $\varphi \in H_0^1(\Omega)$. It is easily checked that (5.2) can be rewritten in the form of our general problem (2.1) with the scalar function Φ given by (2.4).

In our numerical computations we select the quadratic form $a(\cdot, \cdot)$ and the right hand side $\ell(\cdot)$ according to

$$a(v, w) = \int_{\Omega} (\partial_1 v \partial_1 w + \partial_2 v \partial_2 w) \, dx, \quad \ell(v) = 2C \int_{\Omega} v \, dx$$

and the obstacle function is given by $\varphi(x) = \text{dist}(x, \partial\Omega)$, $x \in \Omega$. Finally let $\Omega = (0, 1) \times (0, 1)$.

The resulting obstacle problem (5.2) is modeling the elasto-plastic torsion of a cylindrical bar with cross-section Ω . The active points (where $u(x) = \text{dist}(x, \partial\Omega)$) characterize the plastic region, while the material is considered elastic in inactive points. The solution u represents the stress potential and

the applied twist angle is expressed by the parameter C . We refer for example to Rodrigues [26] for further information.

The inactive region is located along the diagonals of Ω and becomes arbitrarily small with increasing C . This leads to various numerical difficulties so that (5.2) has become a well-established test example [10, 16, 19, 27, 28, 29]. Following [10], we chose the parameter $C = 15$ and the initial triangulation \mathcal{T}_0 as depicted in Figure 5.1.

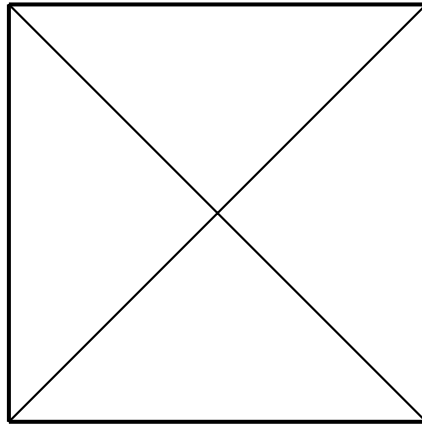


Figure 5.1: Initial Triangulation \mathcal{T}_0

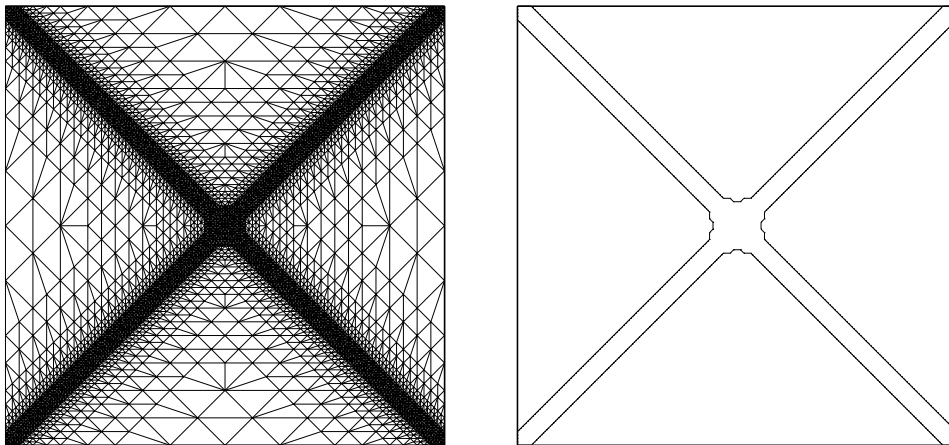


Figure 5.2: Final Triangulation \mathcal{T}_9 and Approximate Free Boundary

Starting with \mathcal{T}_0 , our adaptive algorithm generates a sequence of successively refined triangulations $\mathcal{T}_0, \dots, \mathcal{T}_9$ and of corresponding approximations

$\tilde{u}_0, \dots, \tilde{u}_9$. The final triangulation \mathcal{T}_9 is depicted in the left picture of Figure 5.2. The right picture shows the (discrete) free boundary of the final approximation \tilde{u}_9 . Observe that \mathcal{T}_9 is almost uniformly refined in the inactive region and as coarse as possible in the remaining part of Ω . As the (piecewise linear) obstacle is represented exactly by the finite element approximations, this triangulation is well-suited to the actual problem. The very thin inactive region has no adequate representation on the coarse grids. Even if \mathcal{T}_0 is uniformly refined, all nodal points remain active up to the 3rd refinement level. Hence, the detection and location of the inactive region is a quite challenging task for an adaptive scheme.

The complete approximation history is reported in Table 1. In the fourth column we report the estimates $100 \cdot |e_b^j| / \|\tilde{u}_j\|$ % of the relative approximation errors on the levels $j = 0, \dots, 9$. To check the quality of these error estimates we consider the *effectivity index* κ_j

$$\kappa_j = |e_b^j| / \|u - \tilde{u}_j\|, \quad j = 0, \dots, 9. \quad (5.3)$$

A computable approximation of κ_j is obtained by replacing the exact solution u by the approximation resulting from two further uniform refinements of the final triangulation \mathcal{T}_9 .

Level	Depth	Nodes	est. Error	Effectivity
0	0	1	38.5 %	2.5
1	1	5	38.5 %	2.5
2	2	13	27.4 %	1.8
3	3	53	21.9 %	1.5
4	4	93	17.9 %	1.2
5	5	277	13.5 %	1.0
6	5	357	12.8 %	1.0
7	5	713	10.3 %	1.5
8	6	1577	5.40 %	1.6
9	7	5905	2.81 %	1.7

Table 1. Approximation History

Observe that the resulting effectivity indices can be interpreted as

$$0.39|e_b^j| \leq \|u - \tilde{u}_j\| \leq |e_b^j|, \quad j = 0, \dots, 9,$$

with even better results on the fine levels. Hence, our error estimate works satisfactory throughout the approximation. A comparable a posteriori error estimator [10, 8, 9] fails for this example, because it does not detect the inactive region and thus provides the error estimate zero on the first levels. It is interesting that the approximation history given in Table 1 is very similar to related results in [10] where a considerably more expensive semi-local error estimate has been used.

Example 5.2: A Semidiscrete Stefan Problem The nonlinear evolution equation

$$\frac{\partial}{\partial t} \mathcal{H}(U) - \Delta U = F, \quad \text{in } \Omega \times (0, T), \quad (5.4)$$

with suitable initial and boundary conditions describes the heat conduction in Ω undergoing a change of phase. F is a body heating term and the generalized enthalpy \mathcal{H} is a scalar maximal monotone multifunction,

$$\mathcal{H}(z) = \begin{cases} c_1(z - \theta_0)/k_1 & \text{if } z < \theta_0 \\ [0, L] & \text{if } z = \theta_0, \\ c_2(z - \theta_0)/k_2 + L & \text{if } z > \theta_0 \end{cases} \quad z \in \mathbb{R}, \quad (5.5)$$

which is set-valued at the phase change temperature θ_0 . The unknown generalized temperature U is resulting from the standard Kirchhoff transformation $U = k_1\theta$ for $\theta < \theta_0$ and $U = k_2\theta$ for $U > \theta_0$ of the physical temperature θ . The positive constants $c_i, k_i, i = 1, 2$, describe the thermal properties in the two different phases and $L > 0$ stands for the latent heat.

Discretizing (5.4) in time by the backward Euler scheme with respect to some step size $\tau > 0$, the spatial problems at the different time levels $t_k = k\tau$ can be identified with problems of the form (2.1). The solution $u = U_\tau(\cdot, t_k)$ is the approximation at the actual time step, the bilinear form $a(v, w) = \tau(\nabla v, \nabla w)$ is generated by the Laplacian and the functional ℓ is given by $\ell(v) = (\tau F_k + H_{k-1}, v)$ with $F_k = F(\cdot, t_k)$ and an appropriate selection $H_{k-1} \in \mathcal{H}(U_\tau(\cdot, t_{k-1}))$. Finally, we choose $a_i = c_i/\kappa_i, i = 1, 2$, and $s_1 = 0, s_2 = L$ so that \mathcal{H} is the subdifferential of the piecewise quadratic function Φ defined in (2.5). This semi-discretization has been used to establish existence and uniqueness of a weak solution U (see e.g. Jerome [30]) and also provides a general framework for a variety of numerical methods.

Adaptive techniques for the two-phase Stefan problem have been derived by Nochetto, Paolini, and Verdi [31, 32]. In contrast to our approach which is aiming at the adaptive solution of the spatial problems up to a certain accuracy, their local error indicators concentrate exclusively on an efficient resolution of the free boundary.

We will consider a model problem due to Ciavaldini [33]. The space-time domain $\Omega \times (0, T)$ is given by $\Omega = (0, 1) \times (0, 1)$ and $T = 0.5$. The physical data are $c_1 = 2, k_1 = 1, c_2 = 6, k_2 = 2$ and $\theta_0 = 0, L = 1$. Using the right hand side

$$F(x, t) = \begin{cases} c_1 \exp(-4t) - 4k_1 & \text{if } \theta < 0 \\ c_2 \exp(-4t) - 4k_2 & \text{if } \theta > 0 \end{cases}, \quad x \in \Omega, t > 0,$$

the Kirchhoff transformation U of the physical temperature θ given by

$$\theta(x_1, x_2, t) = (x_1 - 0.5)^2 + (x_2 - 0.5)^2 - \exp(-4t)/4, \quad (x_1, x_2) \in \Omega, t \geq 0,$$

is the exact solution of (5.4) with the corresponding initial and boundary conditions. For the semi-discretization in time we choose the uniform step size $\tau = 0.0125$.

Recall that an estimated accuracy of 5% is required on each time level. We always start with initial triangulation \mathcal{T}_0 as shown in Figure 1.

The evolution of the solution is illustrated in Figure 5.3 showing the discrete interface and the approximate physical solution along the diagonal $x_1 = x_2$ for the first and the last time step. The corresponding final triangulations are depicted in Figure 5.4. In both cases the refinement concentrates on the lack of regularity at the interface.

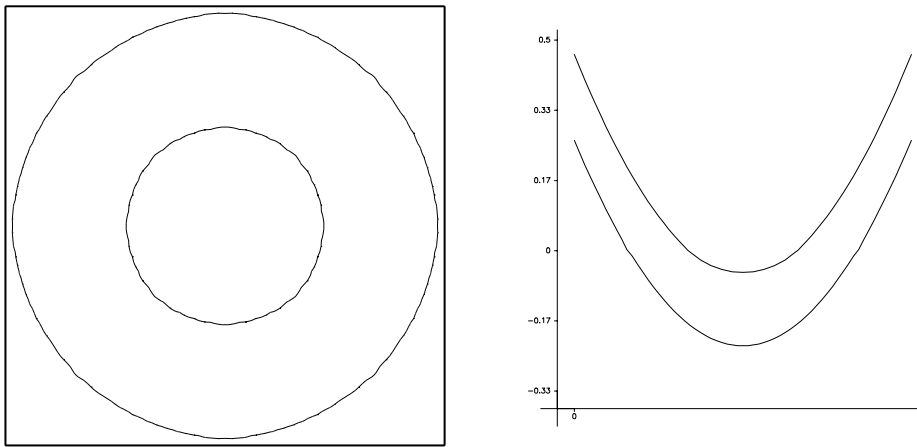


Figure 5.3: Discrete Interfaces and Diagonal Cuts for the First and the Last Time Step

The complete approximation history for the first time step is given in Table 2 where the effectivity rates are computed according to (5.3). On the subsequent time levels we found similar results.

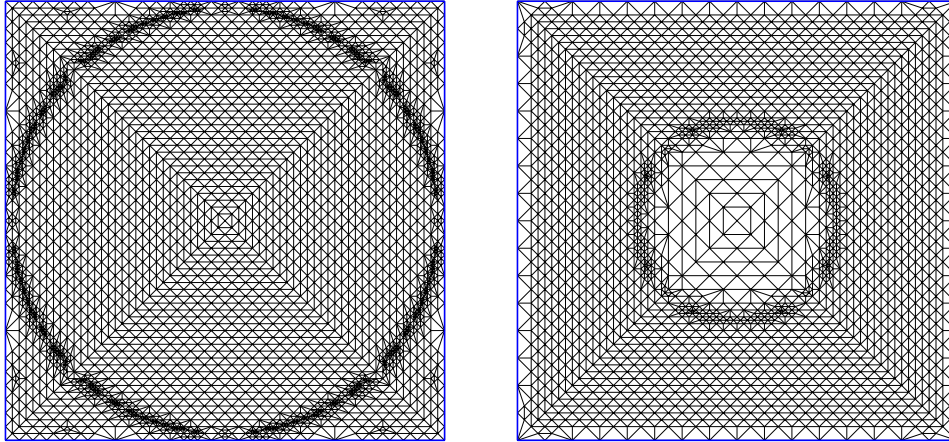


Figure 5.4: Final Triangulations for the First and the Last Time Step

Level	Depth	Nodes	est. Error	Effectivity
0	0	1	160 %	0.14
1	1	5	193 %	0.65
2	2	25	190 %	2.0
3	3	65	56.8 %	0.80
4	4	261	36.7 %	1.8
5	5	409	24.0 %	0.96
6	5	517	17.2 %	0.84
7	6	717	13.1 %	0.90
8	7	1225	7.9 %	0.62
9	7	1629	6.9 %	0.98
10	7	2133	5.9 %	1.0
11	7	3149	4.4 %	0.92

Table 2. Approximation History for the First Time Step

As in the previous example we observe a similar efficiency and reliability of our adaptive algorithm as for related linear selfadjoint problems.

Acknowledgements. The author is deeply indebted to P. Deuffhard and his former colleagues from the Konrad-Zuse-Center in Berlin for numerous fruitful discussions during the preparation of this work. Special thanks to R. Beck and B. Erdmann for invaluable computational assistance and to the referee for important remarks and suggestions.

Bibliography

- [1] O.C. Zienkiewicz, J.P. De S.R. Gago, and D.W. Kelly. The hierarchical concept in finite element analysis. *Computers & Structures*, 16:53–65, 1983.
- [2] P. Deuffhard, P. Leinen, and H. Yserentant. Concepts of an adaptive hierarchical finite element code. *IMPACT Comput. Sci. Engrg.*, 1:3–35, 1989.
- [3] F.A. Bornemann, B. Erdmann, and R. Kornhuber. Adaptive multilevel methods in three space dimensions. *J. Numer. Meth. Engrg.*, 36:3187–3203, 1993.
- [4] F.A. Bornemann, B. Erdmann, and R. Kornhuber. A posteriori error estimates for elliptic problems in two and three space dimensions. *SIAM J. Numer. Anal.*, to appear.
- [5] R. Verfürth. A review of a posteriori error estimation and adaptive mesh-refinement techniques. Manuscript, 1993.
- [6] R. Verfürth. A posteriori error estimation and adaptive mesh-refinement techniques. *J. Comp. Appl. Math.*, 50:67–83, 1994.
- [7] R.E. Bank and R.K. Smith. A posteriori error estimates based on hierarchical bases. *SIAM J. Num. Anal.*, 30:921–935, 1993.
- [8] R. Kornhuber and R. Roitzsch. Self adaptive computation of the breakdown voltage of planar pn-junctions with multistep field plates. In W. Fichtner and D. Aemmer, editors, *Simulation of Semiconductor Devices and Processes*, pages 535–543, Hartung-Gorre, Konstanz, 1991.
- [9] R. Kornhuber and R. Roitzsch. Self adaptive finite element simulation of bipolar, strongly reverse biased pn-junctions. *Comm. Numer. Meth. Engrg.*, 9:243–250, 1993.
- [10] R.H.W. Hoppe and R. Kornhuber. Adaptive multilevel-methods for obstacle problems. *SIAM J. Numer. Anal.*, 31(2):301–323, 1994.
- [11] P. Deuffhard. Cascadic conjugate gradient methods for elliptic partial differential equations. Algorithm and results. In D.E. Keyes and J. Xu, editors, *Proceedings of the 7th International Conference on Domain Decomposition Methods 1993*, pages 29–42, AMS, Providence, 1994.

- [12] V.V. Shaidurov. Some estimates of the rate of convergence for the cascadic conjugate-gradient method. Preprint Nr. 4, Otto-von-Guericke-Universität Magdeburg, 1994.
- [13] F.A. Bornemann and P. Deuffhard. Cascadic multigrid methods for elliptic problems. *Numer. Math.*, submitted.
- [14] J. Crank. *Free and Moving Boundary Problems*. Oxford University Press, Oxford, 1988.
- [15] G. Duvaut and J.L. Lions. *Les inéquations en mécanique et en physique*. Dunaud, Paris, 1972.
- [16] R. Glowinski. *Numerical Methods for Nonlinear Variational Problems*. Springer-Verlag, New York, 1984.
- [17] F. Brezzi, W.W. Hager, and P.A. Raviart. Error estimates for the finite element solution of variational inequalities I. *Numer. Math.*, 28:431–443, 1977.
- [18] C.M. Elliot. Error analysis of the enthalpy method for the Stefan problem. *IMA J. Numer. Anal.*, 7:61–71, 1987.
- [19] R. Kornhuber. Monotone multigrid methods for elliptic variational inequalities I. *Numer. Math.*, 69:167 – 184, 1994.
- [20] R. Kornhuber. Monotone multigrid methods for elliptic variational inequalities II. *Numer. Math.*, to appear.
- [21] R. Kornhuber. Adaptive Monotone Multigrid Methods for Nonlinear Variational Problems. In preparation.
- [22] I. Babuška and W.C. Rheinboldt. Error estimates for adaptive finite element computations. *SIAM J. Numer. Anal.*, 15:736–754, 1978.
- [23] R.E. Bank. *PLTMG – A Software Package for Solving Elliptic Partial Differential Equations, User’s Guide 6.0*. Frontiers in Applied Mathematics. SIAM, Philadelphia, 1990.
- [24] W. Dörfler. Orthogonale Fehlermethoden. Manuscript, 1993.
- [25] R. Beck, B. Erdmann, and R. Roitzsch. KASKADE 3.0 An object-oriented adaptive finite element code. Technical Report TR 95–4, Konrad-Zuse-Zentrum Berlin, 1995.
- [26] J.F. Rodrigues. *Obstacle Problems in Mathematical Physics*. Number 134 in Mathematical Studies. North-Holland, Amsterdam, 1987.

- [27] R. Glowinski, J.L. Lions, and Trémolières. *Numerical Analysis of Variational Inequalities*. North-Holland, Amsterdam, 1981.
- [28] R.H.W. Hoppe. Multigrid algorithms for variational inequalities. *SIAM J. Numer. Anal.*, 24:1046–1065, 1987.
- [29] Y. Kuznetsov, P. Neittaanmäki, and P. Tarvainen. Overlapping block relaxation and Schwarz methods for the obstacle problem with a convection diffusion operator. In D.E. Keyes and J. Xu, editors, *Proceedings of the 7th International Conference on Domain Decomposition Methods 1993*, pages 251–257, AMS, Providence, 1994.
- [30] J.W. Jerome. *Approximation of Nonlinear Evolution Equations*. Academic Press, New York, 1983.
- [31] R. H. Nocchetto, M. Paolini, and C. Verdi. An adaptive finite element method for two-phase Stefan problems in two space dimensions. Part I Stability and error estimates. *Math. Comp.*, 57(195):73–108, 1991.
- [32] R. H. Nocchetto, M. Paolini, and C. Verdi. An adaptive finite element method for two-phase Stefan problems in two space dimensions. Part II Implementation and numerical experiments. *SIAM J. Sci. Stat. Comput.*, 12(5):1207–1244, 1991.
- [33] J.F. Ciavaldini. Analyse numérique d’un problème de Stefan a deux phases par une méthode d’éléments finis. *SIAM J.Numer.Anal.*, 12:464–487, 1975.